

SUPPORTING INFORMATION

HOW TO MEASURE WORK OF ADHESION AND SURFACE TENSION OF SOFT POLYMERIC MATERIALS

Yuan Tian ¹⁾, Maria Ina ²⁾, Zhen Cao ¹⁾, Sergei S. Sheiko^{*2)}, Andrey V. Dobrynin^{*1)}

¹⁾ *Department of Polymer Science, University of Akron, Akron, Ohio 44325, USA*

²⁾ *Department of Chemistry, University of North Carolina, Chapel Hill, North Carolina 27599-3220, USA*

SI.1 SIMULATION DETAILS

Coarse-grained molecular dynamics simulations are used to study interactions of rigid lenses (RL) with elastic substrates (see **Figure S1**). A lens with height h_L is sliced from the spherical particle of radius R_p made of beads arranged into hexagonal closed-packed (HCP) lattice. For small lenses with $R_p < 500\sigma$, each bead is connected with its closest neighbors to form a rigid body; while for large lenses with $R_p = 500\sigma, 1000\sigma$, to reduce computational cost, the lenses are treated as rigid bodies explicitly during simulations (see LAMMPS manual).³ The elastic substrates are made of cross-linked bead-spring chains with the number of monomers $N = 32$. The elastic modulus of the substrate is controlled by changing the degree of cross-linking between chains.

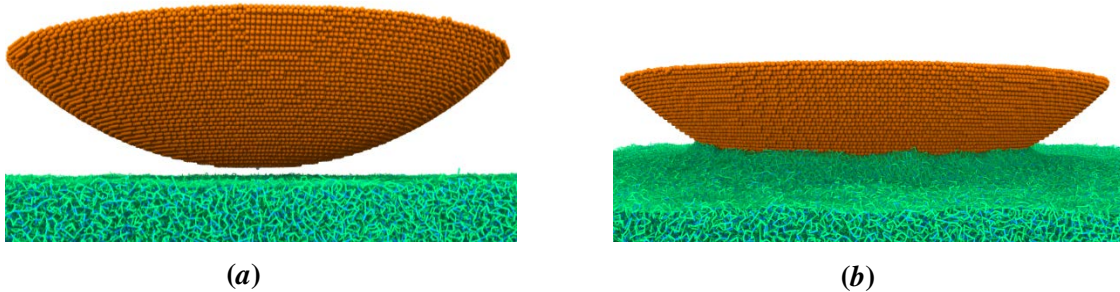


Figure S1: Simulation snapshots of a rigid lens (RL) and an elastic substrate (a) before contact, and (b) in equilibrium state.

In our simulations, the interactions between all beads in a system are modeled by the truncated-shifted Lennard-Jones (LJ) potential¹

$$U_{\text{LJ}} = \begin{cases} 4\epsilon_{\text{LJ}} \left[\left(\frac{\sigma}{r_{\text{lj}}} \right)^{12} - \left(\frac{\sigma}{r_{\text{lj}}} \right)^6 - \left(\frac{\sigma}{r_{\text{cut}}} \right)^{12} + \left(\frac{\sigma}{r_{\text{cut}}} \right)^6 \right] & r \leq r_{\text{cut}} \\ 0 & r > r_{\text{cut}} \end{cases} \quad (\text{SI.1})$$

where r_{ij} is the distance between the i th and j th beads and σ is the bead diameter. The values of the cutoff distance r_{cut} and the value of the LJ-interaction parameter ϵ_{LJ} are summarized in **Table S1**. The connectivity of the beads into polymer chains, the cross-link bonds and bonds belonging to beads forming lenses are modeled by the finite extension nonlinear elastic (FENE) potential²

$$U_{\text{FENE}}(r) = -\frac{1}{2}k_{\text{spring}}R_{\text{max}}^2 \ln\left(1 - \frac{r^2}{R_{\text{max}}^2}\right) \quad (\text{SI.2})$$

with the spring constant $k_{\text{spring}} = 30k_{\text{B}}T/\sigma^2$ and the maximum bond length $R_{\text{max}} = 1.5\sigma$. The repulsive part of the bond potential is given by the LJ-potential with $r_{\text{cut}} = 2^{1/6}\sigma$ and $\epsilon_{\text{LJ}} = 1.5k_{\text{B}}T$.

The elastic substrate made of cross-linked polymer chains is placed on a solid substrate which is modeled by the external potential

$$U(z) = \epsilon_{\text{w}} \left[\frac{2}{15} \left(\frac{\sigma}{z} \right)^9 - \left(\frac{\sigma}{z} \right)^3 \right] \quad (\text{SI.3})$$

where ϵ_{w} is set to $1.0k_{\text{B}}T$. The long-range attractive part of the potential z^{-3} represents the effect of van der Waals interactions generated by the wall half-space.

Table S1 Interaction Parameters

Bead Types	$\epsilon_{\text{LJ}} [k_{\text{B}}T]$	$r_{\text{cut}} [\sigma]$
RL-RL	1.5	2.5
RL-Gel	1.5	2.5
Gel-Gel	1.5	2.5

The system is periodic in x and y directions with system sizes, thickness of rigid lenses (h_L), thickness of the elastic substrate (h_S), total number of atoms (N_{beads}), and total number of bonds (N_{bonds}) are listed in **Table S2**.

Table S2 Systems' Dimensions

$R_p [\sigma]$	$G [k_{\text{B}}T/\sigma^3]$	$h_L [\sigma]$	$L_x = L_y [\sigma]$	$h_S [\sigma]$	N_{beads}	N_{bonds}
36.0	0.498	29.1	143.9	22.9	516,763	1,124,885
60.0		29.3	143.9	22.9	611,557	1,676,372
100.0		29.4	200.0	26.9	1,327,788	3,401,695
200.0		29.0	200.0	53.1	2,687,921	6,812,808
300.0		33.8	240.0	54.3	4,347,099	12,113,118
500.0		34.2	360.0	67.5	9,175,029	17,305,264
1000.0		38.9	560.0	77.8	23,348,492	36,576,599

36.0		29.1	143.9	22.4	516,763	1,165,309
60.0		29.3	143.9	22.4	611,557	1,716,796
100.0		29.4	200.0	26.2	1,327,788	3,306,698
200.0		29.0	200.0	52.8	2,687,921	7,002,802
300.0	0.833	33.8	240.0	37.5	3,374,269	11,057,247
500.0		34.2	360.0	67.5	9,175,029	17,893,164
1000.0		33.7	500.0	73.4	19,253,109	36,695,844

Simulations are carried out in a constant number of particles and temperature ensemble. The constant temperature is maintained by coupling the system to a Langevin thermostat¹ implemented in LAMMPS.³ In this case, the equation of motion of the i th particle has the following form

$$m \frac{d\vec{v}_i(t)}{dt} = \vec{F}_i(t) - \xi \vec{v}_i(t) + \vec{F}_i^R(t) \quad (\text{SI.4})$$

where m is the bead mass set to unity for all particles in a system, $\vec{v}_i(t)$ is the bead velocity, and $\vec{F}_i(t)$ is the net deterministic force acting on the i th bead. The stochastic force $\vec{F}_i^R(t)$ has a zero-average value and δ -functional correlations $\langle \vec{F}_i^R(t) \vec{F}_i^R(t') \rangle = 6k_B T \xi \delta(t-t')$. The friction coefficient ξ is equal to $7.0 m/\tau_{\text{LJ}}$, where τ_{LJ} is the standard LJ-time $\tau_{\text{LJ}} = \sigma(m/k_B T)^{1/2}$. The temperature was kept at $k_B T = 1.0$ in the energetic units. The velocity-Verlet algorithm with a time step $\Delta t = 0.01 \tau_{\text{LJ}}$ was used for integration of the equation of motion. All simulations were performed using LAMMPS.³

At the beginning of the each simulation run, a lens is placed at distance 2.0σ above the surface of an elastic substrate. To accelerate the contact and to reach equilibrium, a strong harmonic spring with $k_{\text{sp}} = 1000 k_B T/\sigma^2$ for small lenses and with $k_{\text{sp}} = 5000 k_B T/\sigma^2$ for large lenses is applied to the center of mass of the lens. The spring is removed after $10^2 \tau_{\text{LJ}}$ for small lenses with $R_p < 500\sigma$ and $10^3 \tau_{\text{LJ}}$ for large lenses with $R_p = 500\sigma$ and 1000σ . This step followed by an equilibration run lasting for $10^4 \tau_{\text{LJ}}$. The equilibrium indentation depth and radius of contact are obtained by averaging the lens' configurations during the final $3 \times 10^3 \tau_{\text{LJ}}$.

Elastic Substrates: The cross-linked substrates are prepared according to simulation procedure described in our previous publication.⁴ The shear moduli of elastic substrates used in current simulations are $G = 0.498 k_B T/\sigma^3$ and $0.833 k_B T/\sigma^3$.

SI.2 EXPERIMENTAL DETAILS

SI.2.1 Substrate Fabrication

The brush-like PDMS elastomers were prepared according to the procedure described in ref [5]. One-step polymerization of monomethacryloxypropyl-terminated poly(dimethylsiloxane) macromonomer (MCR-M11, 1000 g/mol) with different molar ratios of methacryloxypropyl-terminated poly(dimethylsiloxane) (DMS-R18, 5000 g/mol) cross-linker (both materials obtained from Gelest) and *n*-butyl acrylate (*n*BA) allowed preparation of brush elastomers with different cross-link and grafting densities. The formulation contained 56 wt% MCR-M11, 1.5 wt% phenylbis(2,4,6-trimethylbenzoyl)phosphine oxide photo-initiator (BAPO), and 42.5 g of *p*-xylene solvent. To make bottlebrush elastomers ($n_g = 1$) with the shear modulus $G = 3.3$ and 8.1 kPa, the corresponding cross-linker-to-monomer molar ratios were 0.0025 and 0.005, respectively. In the case of the comb elastomers ($n_g = 4$ and 16) with the shear modulus $G = 15.9$ to 54.7 kPa, the molar fractions of *n*BA were 0.252 and 0.063, respectively, the mol fractions of MCR-M11 were 0.746 and 0.935, respectively, and the molar fractions of DMS-R18 were all approximately $1.6 \cdot 10^{-3}$. A mixture was degassed by nitrogen bubbling for 30 minutes before being injected between two glass plates separated by a 0.4 mm spacer. The samples were polymerized under nitrogen at ambient temperature in a UV crosslinking chamber (365 nm UV lamp) for 12 h to yield films.

A linear chain PDMS elastomer with $G=32$ kPa were prepared via the thiolene reaction of vinyl-terminated poly(dimethylsiloxane) (DMS-V22, 9400 g/mol) and (mercaptopropyl)methylsiloxane-dimethylsiloxane copolymer (SMS-022, 6000-8000 g/mol), mixed at a thiol-to-vinyl group molar ratio of 1.5. Solvent (*p*-Xylene) and photo-initiator (BAPO) were added at weight fractions of 20 and 1.5 wt% with respect to the total reaction mixture, respectively. The stiffest substrates, with $G=583.0$ kPa, were prepared using a commercially available silicone composition (Sylgard 184, Dow Corning).

After polymerizations, films were washed with chloroform (2× with enough to immerse and fully swell the films, each time for 8 hrs) in glass Petri dishes. The samples were then deswelled with ethanol as an anti-solvent and dried in an oven at 50 °C. The gel fraction (conversion of monomers to elastomers) was between 90 to 98 wt% in every case.

SI2.2 Substrate Mechanical Properties

Sample elastomers were cut into dog-bone shapes with dimensions of 1.5 mm thickness 2 mm width and a bridge length of 12 mm and were subjected to uniaxial extension at a rate 0.04 mm/s until rupture using an AR-G2 DMA from TA instruments. The corresponding stress-strain curves are given in SI of ref [5].

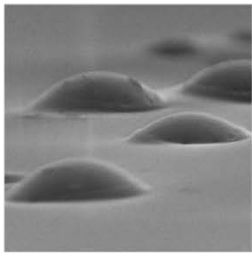
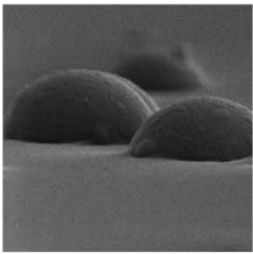
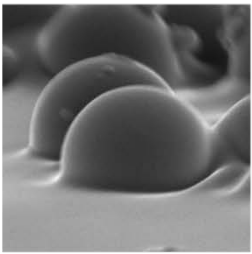
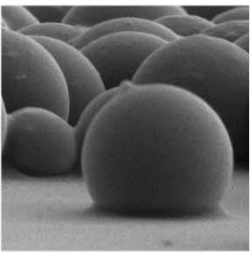
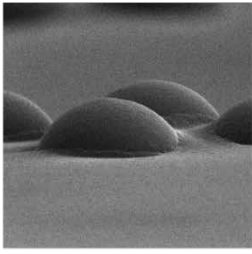
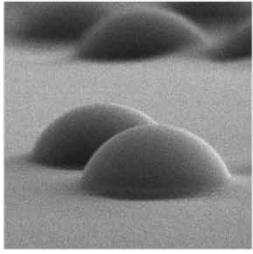
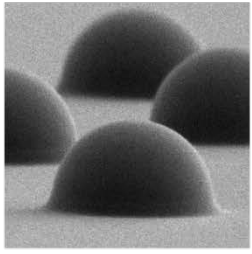
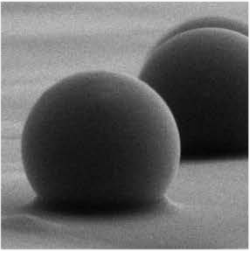
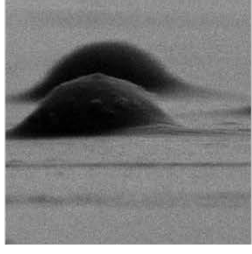
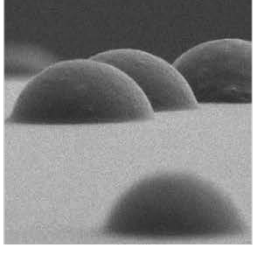
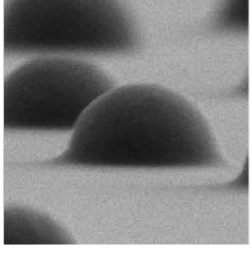
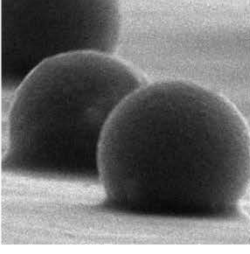
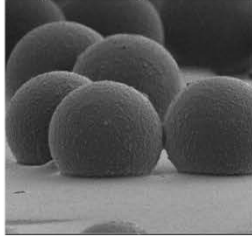
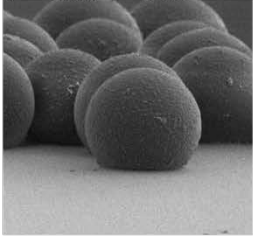
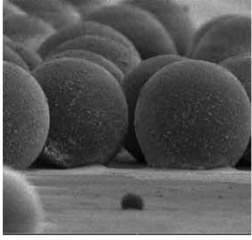
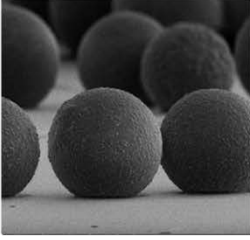
SI2.3 Particle Profile Measurements

Microspheres with radii from 0.225 to 45 μm were used. PS particles with sizes $R_p = 0.225, 0.5, 1.0, 1.3, 1.75 \mu\text{m}$ were produced by a dispersion polymerization in ethanol/water mixture with azobisisobutyronitrile (AIBN) initiator at 70 °C. The particles with sizes $R_p = 3.3, 45 \mu\text{m}$ were purchased from Polysciences, Inc. (PA, USA). PS-COOH particles with sizes $R_p = 0.25, 0.5, 1.0, 1.5, 3, 10 \mu\text{m}$ were purchased from Polysciences, Inc. (PA, USA). Polydisperse PMMA particles with size ranges $R_p = 0.58\text{--}8.38 \mu\text{m}$ were produced by the dispersion polymerization. The particles with $R_p = 10.6\text{--}52.1 \mu\text{m}$ were purchased from Cospheric LLC (CA, USA). **Table S3** lists all particle sizes used in our experiments. To transfer particles into a glass slide they were dispersed in ethanol at a concentration of 0.5 wt% with respect to the particles. The dispersions were spray-coated onto glass coverslips. A finely-cut piece of the elastomer film (3 x 3 mm) was placed on the coverslip for 5 seconds (without pressing) to contact the particles, then it was separated from the glass slide. The film coated with adsorbed particles was left at room temperature (RT) overnight to erase the mechanical history during sample preparation. After annealing, the samples were placed onto copper tapes, coated with a gold-palladium alloy (5 nm) to prevent charging and image distortion, and examined via scanning electron microscopy (FEI Helios 600 Nanolab Dual Beam System) at an acceleration voltage of 5 kV and a beam current of 86 pA. Indentation profiles were quantified in terms of the particle cap height h for each particle using digital image analysis as described in ref [5]. In total, we characterized the behavior of different particle sizes (see **Table S3**) for each of the nine substrate rigidities. The distribution of indentation depths was obtained from measuring the height of the sample set containing 50 particles. We reported the average indentation depth and a standard deviation in each case. For accuracy, we ensured that the substrates were much thicker than the contact radii between the particles and the substrate.

Table S3 Indentation Data

R_p, μm (PS)	G=3.3 kPa		G=8.1 kPa		G=32.0 kPa		G=583 kPa	
	Θ (°)	Δh (μm)	Θ (°)	Δh (μm)	Θ (°)	Δh (μm)	Θ (°)	Δh (μm)
0.225	5	0.41±0.01	5	0.35±0.01	5	0.22±0.02	5	0.09±0.02
0.5	2	0.65±0.02	2	0.62±0.04	2	0.54±0.03	5	0.08±0.03
1	4	1.42±0.04	4	1.37±0.02	4	0.77±0.03	4	0.21±0.06
1.3	5	1.45±0.03	2	1.29±0.04	2	0.99±0.03	2	0.18±0.05
1.75	5	2.11±0.05	5	1.78±0.07	5	1.19±0.06	5	0.21±0.06
3.3	5	3.37±0.02	5	3.14±0.05	5	1.37±0.04	5	0.17±0.06
R_p, μm (PS)	G= 3.3 kPa		G=8.1 kPa		G=15.9 kPa		G=54.7 kPa	
	Θ (°)	Δh (μm)	Θ (°)	Δh (μm)	Θ (°)	Δh (μm)	Θ (°)	Δh (μm)
45	5	13.10±2.08	5	8.68±1.86	2	6.10±1.21	5	2.38±0.58
R_p, μm (PS-COOH)	G=3.3 kPa		G=8.1 kPa		G=32.0 kPa		G=583 kPa	
	Θ (°)	Δh (μm)	Θ (°)	Δh (μm)	Θ (°)	Δh (μm)	Θ (°)	Δh (μm)
0.25	2	0.40±0.01	2	0.29±0.01	2	0.21±0.01	2	0.18±0.03
0.5	0	0.82±0.01	0	0.80±0.01	0	0.75±0.02	5	0.39±0.03
1	5	1.40±0.04	5	1.37±0.04	5	1.19±0.07	5	0.47±0.09
1.5	0	1.87±0.10	2	1.78±0.05	0	1.37±0.05	2	0.48±0.12
3	2	2.76±0.11	2	2.16±0.13	2	1.43±0.07	2	0.59±0.12
10	2	5.55±0.27	2	4.83±0.30	2	2.99±0.25	5	1.65±0.23

R_p , μm (PMMA)	G=3.3 kPa		G=8.1 kPa		G=15.9 kPa		G=32.0 kPa	
	Θ ($^\circ$)	Δh (μm)	Θ ($^\circ$)	Δh (μm)	Θ ($^\circ$)	Δh (μm)	Θ ($^\circ$)	Δh (μm)
10.6	5	6.45 \pm 0.76	5	5.56 \pm 0.44	5	3.72 \pm 0.48	15	2.67 \pm 0.43
10.9	5	6.81 \pm 0.86	5	4.20 \pm 0.43	5	3.59 \pm 0.51		
12.3	5	6.55 \pm 0.65	5	5.09 \pm 0.71	5	4.11 \pm 0.57	15	2.64 \pm 0.50
21.3	5	7.34 \pm 0.50	5	7.53 \pm 0.47	5	6.67 \pm 0.39	5	3.35 \pm 0.18
22.4	5	8.42 \pm 0.36	5	7.72 \pm 0.38	5	5.15 \pm 0.31	5	4.75 \pm 0.25
22.9	5	9.41 \pm 0.57	5	6.56 \pm 0.24	5	5.89 \pm 0.37	5	3.92 \pm 0.22
46.1	10	13.30 \pm 1.01	7	9.79 \pm 1.41	7	7.74 \pm 1.08	5	4.44 \pm 2.41
47.4	10	13.20 \pm 1.65	7	9.01 \pm 1.37	7	5.63 \pm 2.72	5	3.39 \pm 1.52
52.1	10	14.20 \pm 2.31	7	11.9 \pm 0.71	7	7.08 \pm 2.81	5	3.61 \pm 1.78
R_p , μm (PMMA)	G=3.3 kPa		G=8.1 kPa		G=32.0 kPa		G=583 kPa	
	Θ ($^\circ$)	Δh (μm)	Θ ($^\circ$)	Δh (μm)	Θ ($^\circ$)	Δh (μm)	Θ ($^\circ$)	Δh (μm)
0.58	5	0.80 \pm 0.05	5	0.72 \pm 0.08	5	0.56 \pm 0.04	10	0.17 \pm 0.02
0.975	5	1.28 \pm 0.09						
1.01					5	1.00 \pm 0.07		
1.29			5	1.65 \pm 0.10				
1.40					5	1.13 \pm 0.09		
4.28	5	2.89 \pm 0.01						
5.55			5	3.19 \pm 0.12				
8.38	5	4.34 \pm 0.11						

R_p	G=3.3 kPa	G=8.1 kPa	G=32.0 kPa	G=583.0 kPa
SiO ₂ : 1.5 μm				
PS: 1.3 μm				
PS-COOH: 1.5 μm				
R_p	G=3.3 kPa	G=8.1 kPa	G=15.9 kPa	G=32.0 kPa
PMMA: 22.5~23.5 μm				

REFERENCES

1. Frenkel, D.; Smit, B., *Understanding Molecular Simulation: From Algorithms to Applications*. Academic Press: New York, 2001.
2. Kremer, K.; Grest, G. S., Dynamics of entangled linear polymer melts: A molecular - dynamics simulation. *The Journal of Chemical Physics* **1990**, 92 (8), 5057-5086.
3. Plimpton, S., Fast Parallel Algorithms for Short-Range Molecular Dynamics. *Journal of Computational Physics* **1995**, 117 (1), 1-19.
4. Cao, Z.; Stevens, M. J.; Dobrynin, A. V., Adhesion and Wetting of Nanoparticles on Soft Surfaces. *Macromolecules* **2014**, 47 (9), 3203-3209.
5. Ina, M.; Cao, Z.; Vatankehah-Varnoosfaderani, M.; Everhart, M. H.; Daniel, W. F. M.; Dobrynin, A. V.; Sheiko, S. S., From Adhesion to Wetting: Contact Mechanics at the Surfaces of Super-Soft Brush-Like Elastomers. *ACS Macro Letters* **2017**, 6 (8), 854-858.